Phys Chem Minerals (2000) 27: 310–319

ORIGINAL PAPER

K. Matsuzaka · M. Akaogi · T. Suzuki · T. Suda

Mg-Fe partitioning between silicate spinel and magnesiowüstite at high pressure: experimental determination and calculation of phase relations in the system Mg_2SiO_4-Fe_2SiO_4

Received: 18 February 1998 / Revised, accepted: 18 October 1999

Abstract Mg-Fe partitioning experiments between $(Mg,Fe)_2SiO_4$ spinel and (Mg,Fe)O magnesiowüstite were carried out at pressures of 17–21.3 GPa at temperatures of 1400 and 1600 °C, using a multi-anvil apparatus, in order to determine interaction parameters of spinel and magnesiowüstite solid solutions and also to constrain the equilibrium boundaries of the postspinel transition in the Fe-rich side in the system Mg_2SiO_4-Fe_2SiO_4. The obtained values of the interaction parameters were 3.4 ± 1.5 and 13.9 ± 1.4 kJ mol^{-1}, respectively, for spinel and magnesiowüstite solid solutions at 19 GPa and 1600 °C. The partitioning data in the system Mg_2SiO_4-Fe_2SiO_4 at 1400 and 1600 °C showed that the transition boundary between spinel and the mixture of magnesiowüstite and stishovite has a negative dP/dT slope. Using the above interaction parameters and available thermodynamic data of the Mg_2SiO_4 and Fe_2SiO_4 end members, the transition boundaries of spinel to the mixture of magnesiowüstite and stishovite were calculated. Within the uncertainties of the data used, the calculated boundaries are in good agreement with the boundaries at 1400 and 1600 °C experimentally determined in this study. The dissociation boundary of Fe_2SiO_4 spinel to wüstite and stishovite, calculated from the thermodynamic data, has a negative slope of −1.5 ± 0.6 MPa K^{-1}.

Key words Element partitioning · High pressure phase relation · Mixing property · Spinel · Magnesiowüstite

K. Matsuzaka · M. Akaogi (✉) · T. Suzuki · T. Suda
Department of Chemistry,
Gakushuin University, 1-5-1, Mejiro,
Toshima-ku, Tokyo 171-8588, Japan
Fax: 81-3-5992-1029

Present address:
K. Matsuzaka
Disco Co., Higashikojiya, Ohta-ku, Tokyo 144-0033, Japan

Introduction

High-pressure phase relations in the system MgO-FeO-SiO_2 are of great importance in understanding the chemistry and mineralogy of the earth's mantle, and experimental and theoretical studies of the phase relations have been extensively carried out. Among the high-pressure phase relations of ferromagnesian silicates, the postspinel transformation in the system Mg_2SiO_4-Fe_2SiO_4 has received special attention, because it has been widely considered that this transition could be responsible for the 660-km seismic discontinuity which separates the upper and lower mantle.

Ito and Takahashi (1989) studied in detail the phase relations of the postspinel transitions in the system Mg_2SiO_4-Fe_2SiO_4 by high-pressure experiments using a multianvil apparatus. They demonstrated that Mg_2SiO_4-rich $(Mg,Fe)_2SiO_4$ spinel dissociates into $(Mg,Fe)SiO_3$ perovskite and (Mg,Fe)O magnesiowüstite, in contrast to spinel dissociation into magnesiowüstite and stishovite in the Fe_2SiO_4-rich side. They determined the postspinel phase relations in the compositional range of about 40–100 mol% Mg_2SiO_4. However, the experimental determination of the phase relations in the whole compositional range is needed for fully understanding the postspinel transitions in the Mg_2SiO_4-Fe_2SiO_4 system. In the Fe-rich compositions in the system Mg_2SiO_4-Fe_2SiO_4, we determined the compositions of coexisting spinel and magnesiowüstite at 18.5 and 20.4 GPa at 1600 °C (Akaogi et al. 1998). However, our experimental data were insufficient to constrain the whole boundaries of the transition, and also the temperature dependence of the boundaries has not yet been examined.

Fei et al. (1991) carried out Mg-Fe partition experiments between spinel and magnesiowüstite at 15 GPa and 1500 °C to constrain the mixing properties of the coexisting phases which were used for thermodynamic calculation of the transition boundaries. However, their experimental data were limited to only Fe-rich

composition. Therefore, it is highly desirable to perform the Mg-Fe partitioning experiments in the whole compositional range of Mg-Fe solid solutions to derive the interaction parameters.

In this study, we performed the Mg-Fe partitioning experiments in the system Mg_2SiO_4-Fe_2SiO_4 between spinel and magnesiowüstite to constrain tightly the transition boundaries from spinel to the mixture of magnesiowüstite and stishovite in the compositions of 50–90 mol% Fe_2SiO_4 at 17.2–21.3 GPa, using a multianvil apparatus. The experiments were carried out at two different temperatures, 1400 and 1600 °C, to determine the temperature dependence of the phase boundaries. Special care was taken to obtain the equilibrium compositions. For the compositional range of 20–80 mol% Fe_2SiO_4, we also carried out partitioning experiments between spinel and magnesiowüstite to obtain the partition coefficients at 17–19 GPa and 1600 °C. These results include the partition coefficients in complementary Mg-rich composition to the former experiments in the Fe_2SiO_4-rich side. The partition data in the whole compositional range have been used to elucidate the mixing parameters of spinel and magnesiowüstite solid solutions by the least-squares method. Using the obtained mixing properties of the solid solutions and currently available thermodynamic data of the end members, we calculated the transition boundaries of spinel to magnesiowüstite and stishovite to compare with those by experimental determinations. Finally, the dissociation boundary of Fe_2SiO_4 spinel to wüstite and stishovite was calculated and compared with those in the previous studies.

Experimental procedures

Starting materials

Forsterite, fayalite, olivine solid solutions in the system Mg_2SiO_4-Fe_2SiO_4, periclase, and magnesiowüstite solid solution were used as starting materials. Reagent-grade chemicals were used throughout. Forsterite was synthesized from a mixture of MgO and silicic acid (SiO_2 11 wt% H_2O) by heating at 1600 °C for 60 h. Fayalite was made from a mixture of Fe_2O_3 and silicic acid by heating for 30 h in a controlled oxygen fugacity using mixed gas flow of H_2, CO_2, and Ar with 1:1:2 volumetric ratios. $(Mg_x,Fe_{1-x})_2SiO_4$ olivine solid solutions (x = 0.1, 0.2, 0.4, and 0.5) were synthesized from mixtures of forsterite and fayalite with the above ratios at 1190–1350 °C for a total heating time of about 55 h in the same gas mixture as fayalite. In the sintering experiments, the heated samples were quenched, ground, pelletized, and heated again, and this cycle was repeated three times for each sample in order to make homogeneous olivine solid solutions. Magnesiowüstite solid solution was made from an equimolar mixture of MgO and Fe_2O_3 by heating at 1500 °C for 15 h in the controlled oxygen fugacity using the same gas mixture as for olivine solid solutions.

The synthesized forsterite, fayalite, olivine solid solutions, and magnesiowüstite were examined by powder X-ray diffraction method, confirming single-phase materials. EPMA analysis showed that all the synthesized materials were stoichiometric and that the olivine solid solutions and magnesiowüstite were almost homogeneous in composition: Mg_2SiO_4 mol% of the four olivine solid solutions was 10.8 ± 0.3, 20.7 ± 0.5, 41.0 ± 0.4, and 51.0 ± 0.9, and MgO mol% of magnesiowüstite was 33.1 ± 0.3, where the errors represent one standard deviation.

Two different types of starting materials, A and B, were used for the high-pressure phase equilibrium experiments. Type A, with olivine composition, was further divided into two sorts: olivine solid solutions of the above four different compositions, and the mixtures of Mg_2SiO_4 forsterite and Fe_2SiO_4 fayalite with molar ratios of 10:90, 20:80, 40:60, and 50:50. Type B starting material was a mixture of forsterite, fayalite, and periclase or $(Mg_{0.33},Fe_{0.67})O$ magnesiowüstite, where the molar ratio of forsterite + fayalite: magnesiowüstite (or periclase) was 1:3. A mixture of $(Mg_{0.41},Fe_{0.59})_2SiO_4$ olivine solid solution and metallic iron of about 5 wt% was also used as a starting material to keep the oxygen fugacity of the sample in equilibrium with the metallic iron. Using this starting material, the partitioning experiment was made to examine whether the Mg-Fe partition coefficient between spinel and magnesiowüstite was changed or not due to change of oxygen fugacity with or without coexisting metallic iron.

High pressure experiments

A split-cylinder type multianvil apparatus was used for the high-pressure experiments at Gakushuin University. Eight tungsten carbide anvils with a truncated edge length of 2.5 mm were used in combination with a semisintered 7-mm edged MgO octahedron containing 5 wt% Cr_2O_3. A lanthanum chromite sleeve 3.0 mm in outer diameter and 1.5 mm in inner diameter was placed in the MgO octahedron as a thermal insulator, and both of them were heated at 750 °C overnight to remove possible absorbed water. A rhenium tubular heater 30 μm thick was inserted into the lanthanum chromite sleeve and used as a heater/capsule. Starting material was put into the capsule. Two lanthanum chromite plugs 1.3 mm in diameter and 1.0 mm in length were put in both ends of the heater for thermal insulation. Two platinum disks 30 μm thick were inserted between the plugs and the sample to avoid reaction between them. Temperature was measured on the outer surface of the central part of the heater using a Pt/Pt-13%Rh thermocouple 0.1 mm in diameter. No correction was made for pressure effect on emf of the thermocouple.

Pressure calibration was made at room temperature, using transitions of Bi I-II (2.55 GPa), Bi III-V (7.7 GPa), ZnS (15.5 GPa), GaAs (18.3 GPa), and GaP (23 GPa). Pressures at 1400 and 1600 °C were further calibrated, based on Katsura and Ito's (1989) pressures of α-β and β-γ transitions of Mg_2SiO_4, 14.6 and 19.9 GPa, respectively, at 1400 °C, and 15.0 and 20.8 GPa, respectively, at 1600 °C. The relative uncertainty in pressure was estimated to be smaller than ±0.2–0.3 GPa, and the uncertainty in absolute value of pressure was presumed to be about ±0.5 GPa. The sample was kept at 17–21.3 GPa at 1400 and 1600 °C for 10–300 min. In the high-pressure high-temperature runs, we first applied pressure, and subsequently increased temperature. The sample was kept at the desired P,T conditions for a period of time, and then quenched isobarically and recovered at ambient conditions. Temperature gradient in the furnace was not measured, but was estimated to be around 0.1 °C μm^{-1} along the long axis of the sample in the central part where EPMA analysis of spinel and magnesiowüstite was made.

Phase identification was made by powder X-ray diffraction, using a part of the sample in the central part of the capsule. The remaining sample was polished, and examined by microscopic observation, microfocus X-ray diffraction, and backscattered electron image of EPMA. Grain size of the phases in the run products longer than about 1 h was typically about 20–40 μm for spinel, 5–20 μm for magnesiowüstite, and 2–10 μm for stishovite. In the central part of each run product, spinel and magnesiowüstite grains more than 50–100 μm distant from the Re capsule were analyzed by means of EPMA, and the compositions in each run were determined from the average of 10–33 analysis points with standard deviation. The accelerating voltage and the beam current were 15 kV and 12 nA, respectively, and the beam diameter was about 1 μm. Standard materials for the EPMA analysis were periclase for Mg, hematite for Fe, and wollastonite for Si. The compositions were calculated using the Bence-Albee correction method.

Results and discussion

Mg-Fe partitioning data and spinel dissociation boundaries

Table 1 summarizes the results of the high-pressure high-temperature experiments. The phases observed were spinel, magnesiowüstite, and stishovite in the run products using type A starting materials, and spinel and magnesiowüstite for type B. In run no. A31, metallic iron added in the starting material was also observed in the run product. Table 2 shows results of EPMA analyses of spinel and magnesiowüstite in some typical run products. The results show that magnesiowüstite appeared to contain SiO_2 of about 0.5–1 wt%. However, it was interpreted that the SiO_2 content in magnesiowüstite was caused by beam overlap with adjacent spinel, because of its small grain size. Calculation showed that by the beam overlap the 100 Mg/(Mg + Fe) value of magnesiowüstite was changed by only a very small amount, mostly within its standard deviation. Therefore, we did not correct this contamination effect on the partitioning data.

Figure 1 shows the compositions of coexisting spinel and magnesiowüstite as a function of run time in the runs with the bulk composition of 40–41 mol% Mg_2SiO_4 at 20.4 GPa and 1600 °C. In the runs using the starting material of $(Mg_{0.41},Fe_{0.59})_2SiO_4$ olivine solid solution, the 100 Mg/(Mg + Fe) values in spinel and magnesiowüstite diverged from the starting ratio with increasing time. The compositions were considerably scattered within the initial 30 min. However, the compositions of spinel and magnesiowüstite became less

Table 1 Results of the Mg-Fe partitioning experiments between spinel and magnesiowüstite. *Sp* Spinel; *Mw* magnesiowüstite; *St* stishovite

Run no.[a]	Starting material[b]	Pressure (GPa)	Time (min)	Phases	100 Mg/(Mg + Fe)[d]	
					Sp	Mw
Temperature = 1400 °C						
A20	$Fo_{11}Fa_{89}$	17.9	300	Sp + Mw + St	15.2 ± 0.9	3.5 ± 0.6
A21	10Fo + 90Fa	17.9	180	Sp + Mw + St	15.2 ± 0.7	3.8 ± 0.5
A22	10Fo + 90Fa	17.9	300	Sp + Mw + St	16.0 ± 1.4	3.9 ± 0.5
A23	$Fo_{21}Fa_{79}$	19.8	300	Sp + Mw + St	39.6 ± 1.0	12.6 ± 1.5
A24	20Fo + 80Fa	19.8	180	Sp + Mw + St	39.7 ± 0.9	12.3 ± 0.9
A25	20Fo + 80Fa	19.8	300	Sp + Mw + St	39.7 ± 1.0	11.8 ± 0.9
A26	$Fo_{41}Fa_{59}$	21.0	180	Sp + Mw + St	50.4 ± 1.0	19.6 ± 1.0
A28	40Fo + 60Fa	21.0	90	Sp + Mw + St	54.2 ± 0.5	21.5 ± 1.1
A29	40Fo + 60Fa	21.0	300	Sp + Mw + St	51.5 ± 0.5	17.7 ± 0.6
Temperature = 1600 °C						
A1	$Fo_{11}Fa_{89}$	17.2	180	Sp + Mw + St	12.3 ± 0.5	2.6 ± 0.5
A3	10Fo + 90Fa	17.2	60	Sp + Mw + St	14.3 ± 1.3	3.4 ± 0.4
A4	10Fo + 90Fa	17.2	220	Sp + Mw + St	13.1 ± 1.1	3.2 ± 0.4
A6[c]	$Fo_{21}Fa_{79}$	18.5	180	Sp + Mw + St	30.3 ± 1.0	8.9 ± 0.6
A7[c]	20Fo + 80Fa	18.5	60	Sp + Mw + St	31.6 ± 0.6	8.6 ± 0.6
A8[c]	20Fo + 80Fa	18.5	300	Sp + Mw + St	30.8 ± 1.0	8.5 ± 0.6
A9[c]	$Fo_{41}Fa_{59}$	20.4	10	Sp + Mw + St	45.2 ± 0.9	25.5 ± 8.1
A10	$Fo_{41}Fa_{59}$	20.4	30	Sp + Mw + St	46.2 ± 0.7	17.3 ± 1.5
A11[c]	$Fo_{41}Fa_{59}$	20.4	60	Sp + Mw + St	48.6 ± 0.8	20.0 ± 0.7
A12	$Fo_{41}Fa_{59}$	20.4	180	Sp + Mw + St	47.2 ± 0.9	17.0 ± 1.1
A13[c]	$Fo_{41}Fa_{59}$	20.4	300	Sp + Mw + St	47.9 ± 0.4	15.1 ± 1.3
A14[c]	40Fo + 60Fa	20.4	60	Sp + Mw + St	47.5 ± 0.6	15.1 ± 0.7
A15[c]	40Fo + 60Fa	20.4	300	Sp + Mw + St	48.0 ± 0.5	14.8 ± 0.7
A31	$Fo_{41}Fa_{59}$ + 5 wt% Fe	20.4	300	Sp + Mw + St + Fe	45.4 ± 0.4	15.5 ± 1.6
A16	$Fo_{51}Fa_{49}$	21.3	180	Sp + Mw + St	54.6 ± 0.9	21.6 ± 0.9
A17	50Fo + 50Fa	21.3	10	Sp + Mw + St	54.6 ± 1.5	19.6 ± 1.0
A18	50Fo + 50Fa	21.3	180	Sp + Mw + St	55.3 ± 1.2	21.3 ± 1.6
A19	50Fo + 50Fa	21.3	300	Sp + Mw + St	55.1 ± 0.6	19.7 ± 0.8
B8	25Fa + $75Pe_{33}Wü_{67}$	17.0	300	Sp + Mw	35.8 ± 0.3	11.2 ± 0.1
B6	12.5Fo + 12.5Fa + $75Pe_{33}Wü_{67}$	17.0	300	Sp + Mw	60.5 ± 0.4	28.6 ± 0.6
B10	25Fo + $75Pe_{33}Wü_{67}$	17.0	300	Sp + Mw	73.3 ± 0.2	50.9 ± 0.4
B13	5Fo + 20Fa + $75Pe_{33}Wü_{67}$	19.0	300	Sp + Mw	49.5 ± 0.4	16.9 ± 0.4
B3	12.5Fo + 12.5Fa + $75Pe_{33}Wü_{67}$	19.0	300	Sp + Mw	60.7 ± 0.4	27.4 ± 0.4
B9	25Fo + $75Pe_{33}Wü_{67}$	19.0	300	Sp + Mw	75.5 ± 0.4	50.8 ± 0.6
B1	12.5Fo + 12.5Fa + $75Pe_{100}$	19.0	300	Sp + Mw	85.4 ± 0.4	76.2 ± 0.8

[a] Run numbers with A and B show the runs using starting materials of the type A and B, respectively. See text

[b] xFo + yFa + (100 − x − y)Mw represents the mechanical mixture of x mol% forsterite, y mol% fayalite, and (100 − x − y) mol% magnesiowüstite. Fo_xFa_{100-x} represents the olivine solid solution of x mol% Mg_2SiO_4 and (100 − x) mol% Fe_2SiO_4. Pe_x-$Wü_{100-x}$ shows the magnesiowüstite solid solution of x mol% MgO and (100−x) mol% FeO

[c] Data shown in Akaogi et al. (1998)

[d] Error is standard deviation

Table 2 Results of EPMA analyses of spinel and magnesiowüstite in some run products. The *values in parentheses* represent standard deviation which refers to the last digit(s). The *number in brackets* is number of analysis points. Numbers of atoms for magnesiowüstite and spinel are based on the formulas with one and four oxygens, respectively. *Sp* Spinel; *Mw* magnesiowüstite

Run no.	B1		B3		B6		B9	
	Sp [33]	Mw [27]	Sp [28]	Mw [22]	Sp [30]	Mw [26]	Sp [31]	Mw [28]
SiO_2	39.17(31)	0.46(42)	36.01(35)	0.76(4)	35.47(44)	1.13(7)	37.95(38)	0.83(13)
MgO	45.90(53)	62.54(179)	29.99(41)	16.87(25)	29.68(45)	17.51(50)	39.42(34)	35.39(60)
FeO	13.99(34)	34.88(76)	34.60(29)	79.73(60)	34.54(33)	77.86(34)	22.81(35)	61.16(68)
Total	99.06(63)	97.88(154)	100.60(75)	97.36(55)	99.70(92)	96.50(58)	100.19(64)	97.38(58)
Si	0.988(7)	0.003(3)	0.989(10)	0.008(0)	0.985(12)	0.012(0)	0.987(10)	0.008(1)
Mg	1.727(19)	0.756(21)	1.228(17)	0.269(4)	1.228(19)	0.279(8)	1.529(13)	0.500(9)
Fe	0.295(7)	0.236(5)	0.794(7)	0.714(5)	0.802(8)	0.697(3)	0.496(8)	0.485(5)
100 Mg/(Mg + Fe)	85.4(4)	76.2(8)	60.7(4)	27.4(4)	60.5(4)	28.6(6)	75.5(4)	50.8(6)

scattered in the runs after 1 h, and were unchanged after 3 h. In the runs using the mixture of forsterite and fayalite with a molar ratio of 40:60, the 100 Mg/(Mg + Fe) of spinel and magnesiowüstite changed closer to each other and became unchanged after 1 h. As shown in Fig. 1 and Table 1, the final compositions agreed within the errors between the two kinds of starting materials. It was concluded that the compositions of spinel and magnesiowüstite were very close to equilibrium, when the following two criteria were satisfied, i.e., the compositions were not changed with run time and were consistent in both kinds of starting materials. Thus, the averages of the two final compositions were regarded as the equilibrium compositions in the experiments using type A starting materials, and are shown in Table 3. The run time required for equilibration was about 3 h at 1400 and 1600 °C. The experiments using type B starting materials were made at 1600 °C for 5 h. Therefore, the resultant compositions of spinel and magnesiowüstite were also seen to be very close to equilibrium, and are shown in Table 3.

When we compare the results of the run containing 5 wt% metallic iron (run no. A31) with those without the additional iron (run nos. A12, A13, and A15), all of which were made under the same P,T conditions, the compositions of magnesiowüstite agreed within the errors and those of spinel were consistent within about 2 mol%, which was similar in size to the above compositional difference between the two kinds of starting materials. The partition coefficients (defined below) agreed within the errors in the runs with and without metallic iron. These results suggest that oxygen fugacity in the runs without metallic iron was very similar to that on adding metallic iron.

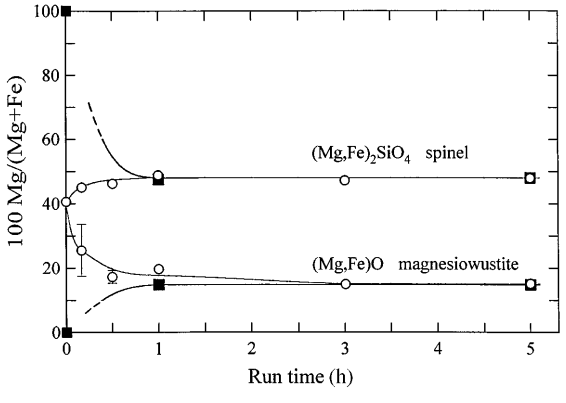

Fig. 1 Relationship between run time and 100 Mg/(Mg + Fe) values of spinel and magnesiowüstite in the runs at 20.4 GPa and 1600 °C. *Circles* represent the compositions in the runs using the starting material of $(Mg_{0.41},Fe_{0.59})_2SiO_4$ olivine solid solution. *Squares* show the values in the runs using the starting material of the mixture of forsterite and fayalite with 40:60 molar ratio. *A circle and squares at 0 h* are the values of the starting materials

Table 3 shows the equilibrium compositions obtained above and partition coefficients defined by

$$K_D = \left(X_{Fe}^{sp}/X_{Mg}^{sp}\right) \Big/ \left(X_{Fe}^{mw}/X_{Mg}^{mw}\right) , \quad (1)$$

where X_{Mg}^{sp} is the mole fraction of the Mg_2SiO_4 component in $(Mg,Fe)_2SiO_4$ olivine, and X_{Mg}^{mw} is the mole fraction of the MgO component in (Mg,Fe)O magnesiowüstite. We assume that all the iron in spinel and magnesiowüstite was ferrous in all the run products. As shown in Table 2, the compositions of spinel and magnesiowüstite which were close to stoichiometric support this assumption. Recent multianvil experiments also showed that ferric iron content in magnesiowüstite was decreased to a very small amount and was relatively independent of oxygen fugacity at high pressure around 20 GPa (McCammon et al. 1998). Figure 2 illustrates the equilibrium compositions and thereby constrained transition boundaries from spinel to the mixture of magnesiowüstite and stishovite at 1400 and 1600 °C. This figure shows that the transition boundary shifts to lower pressure with increasing temperature and the pressure difference between the boundaries at 1400 and 1600 °C increases with increase in the Fe_2SiO_4 component in the bulk composition. This suggests that dissociation pressure of Fe_2SiO_4 spinel to wüstite and stishovite decreases with increasing temperature, indicating a negative dP/dT boundary.

Figure 3 compares the transition boundaries at 1600 °C between our work and those of the previous studies by Ito and Takahashi (1989) and Fei et al. (1991). Our boundary in Fig. 3 is placed by about 1.5–2.5 GPa higher than that by Fei et al.'s (1991)

Table 3 Equilibrium compositions of spinel and magnesiowüstite and Mg-Fe partition coefficients

Pressure (GPa)	Temperature (°C)	100 X_{Mg}^{sp}	100 X_{Mg}^{mw}	K_D^a
17.9	1400	15.6 ± 0.8	3.7 ± 0.4	0.208 ± 0.027
19.8	1400	39.6 ± 0.7	12.2 ± 0.9	0.212 ± 0.019
21.0	1400	51.0 ± 0.6	18.7 ± 0.6	0.221 ± 0.010
17.2	1600	12.7 ± 0.6	2.9 ± 0.3	0.205 ± 0.025
18.5	1600	30.5 ± 0.7	8.7 ± 0.4	0.217 ± 0.013
20.4	1600	47.9 ± 0.3	15.0 ± 0.7	0.192 ± 0.011
21.3	1600	54.9 ± 0.5	20.6 ± 0.6	0.213 ± 0.009
17.0	1600	35.8 ± 0.3	11.2 ± 0.1	0.226 ± 0.004
17.0	1600	60.5 ± 0.4	28.6 ± 0.6	0.262 ± 0.009
17.0	1600	73.3 ± 0.2	50.9 ± 0.4	0.378 ± 0.007
19.0	1600	49.5 ± 0.4	16.9 ± 0.4	0.208 ± 0.007
19.0	1600	60.7 ± 0.4	27.4 ± 0.4	0.244 ± 0.006
19.0	1600	75.5 ± 0.4	50.8 ± 0.6	0.334 ± 0.011
19.0	1600	85.4 ± 0.4	76.2 ± 0.8	0.547 ± 0.030

[a] $K_D = (X_{Fe}/X_{Mg})^{Sp}/(X_{Fe}/X_{Mg})^{Mw}$

thermodynamic calculation. Probably this difference can be explained as follows. Yagi et al. (1979) and Ohtani (1979) reported the pressure of about 17 ± 1 GPa at around 1000 °C for dissociation of Fe_2SiO_4 spinel into wüstite and stishovite, and Fei et al. (1991) used this value to constrain the thermodynamic data. They also used thermodynamic data on stishovite by Akaogi and Navrotsky (1984), which were substantially different from new, precise determinations (Akaogi et al. 1995; Liu et al. 1996) and gave a strongly negative dP/dT slope for the dissociation of Fe_2SiO_4 spinel. As a result, Fei et al.'s (1991) dissociation pressure of Fe_2SiO_4 spinel decreased to 13.8 GPa at 1600 °C, which is about 2.5 GPa lower than in our study. Our boundary, extrapolated to about 22 GPa, is close to that in Ito and Takahashi's experiments. This general consistency is presumably due to the fact that our experiments were made with a pressure calibration method very similar to that of Ito and Takahashi. A small difference between Ito and Takahashi's boundary and ours is observed at about 22 GPa. This may be explained by the fact that only a few runs were made to constrain the boundary in Ito and Takahashi's study at this pressure region.

Thermodynamic analysis of Mg-Fe partitioning data

The Mg-Fe partitioning equilibrium between spinel and magnesiowüstite is expressed as the following exchange reaction,

$$1/2Mg_2SiO_4(sp) + FeO(mw) = 1/2Fe_2SiO_4(sp) + MgO(mw)\ . \qquad (2)$$

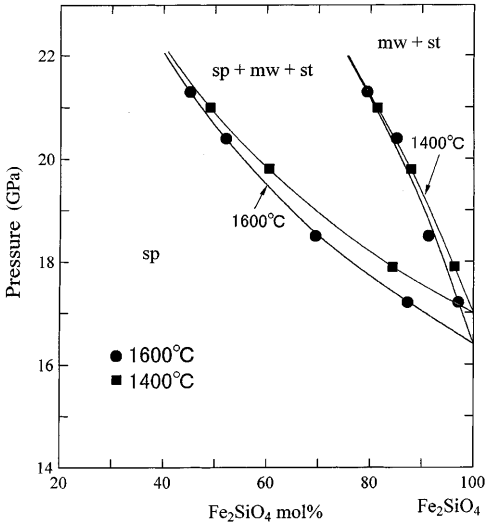

Fig. 2 The equilibrium compositions of coexisting spinel and magnesiowüstite and the transition boundaries of spinel to magnesiowüstite and stishovite in the system Mg_2SiO_4-Fe_2SiO_4 at 1400 and 1600 °C. *Squares* show the composition of spinel and magnesiowüstite at 1400 °C, and *circles* at 1600 °C; *sp* spinel; *mw* magnesiowüstite; *st* stishovite

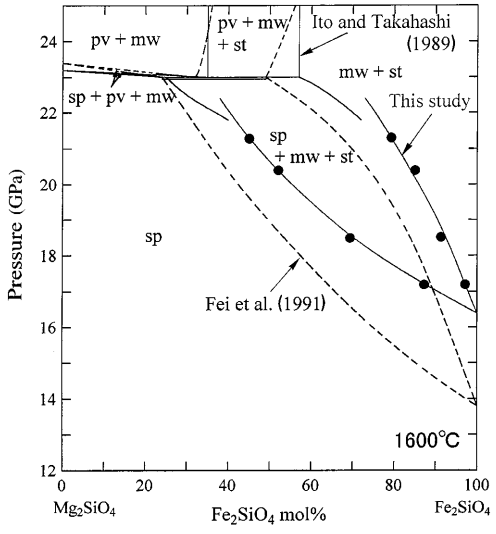

Fig. 3 Comparison of the transition boundary experimentally determined in this study with that by Ito and Takahashi's (1989) experiments and by Fei et al.'s (1991) thermodynamic calculation. All the boundaries are at 1600 °C. *Circles* represent compositions of spinel and magnesiowüstite determined in this study; *sp* spinel; *mw* magnesiowüstite; *st* stishovite; *pv* perovskite

We have at the equilibrium

$$1/2\mu^{sp}_{Mg_2SiO_4} + \mu^{mw}_{FeO} = 1/2\mu^{sp}_{Fe_2SiO_4} + \mu^{mw}_{MgO} \ , \quad (3)$$

where μ_i^A is partial molar free energy of i component in phase A. The μ_i^A is expressed as

$$\mu_i^A = \mu_i^{\circ A} + RTln\ a_i^A \ , \quad (4)$$

where a_i^A is activity of i component in phase A, and $\mu_i^{\circ A}$ is molar free energy of pure i component with the structure of phase A. We take the standard state of all components to be pure phases at the pressure and temperature of interest. Then, by substituting Eq. (4) into Eq. (3), we have

$$\Delta G^\circ = -RTln\left[\left(a^{sp}_{Fe_2SiO_4}\right)^{1/2} a^{mw}_{MgO} \Big/ \left(a^{sp}_{Mg_2SiO_4}\right)^{1/2} a^{mw}_{FeO}\right] \ , \quad (5)$$

where ΔG° is standard free energy difference for Eq. (2) at the pressure and temperature of interest. The activities in spinel and magnesiowüstite are expressed, respectively, by

$$a_i^{sp} = \left(X_i^{sp}\gamma_i^{sp}\right)^2 \quad (6)$$

$$a_j^{mw} = X_j^{mw}\gamma_j^{mw} \ , \quad (7)$$

where X_i^{sp} and γ_i^{sp} are mole fraction and activity coefficient, respectively, of the i(=Mg_2SiO_4, Fe_2SiO_4) component in $(Mg,Fe)_2SiO_4$ spinel solid solution, and X_j^{mw} and γ_j^{mw} are mole fraction and activity coefficient, respectively, of the j(=MgO, FeO) component in (Mg,Fe)O magnesiowüstite solid solution. In this study, we adopt a symmetric regular solution model for both spinel and magnesiowüstite solid solutions (Thompson 1967). Then, the activity coefficient is expressed as:

$$RTln\ \gamma_i^A = (1 - X_i^A)^2 W_G^A \ , \quad (8)$$

where W_G^A is interaction parameter of phase A for one cation site basis.

By substituting Eqs. (6)–(8) into Eq. (5), we have

$$-RTln\ K_D = \Delta G^\circ + W_G^{sp}(2X^{sp}_{Mg} - 1) - W_G^{mw}(2X^{mw}_{Mg} - 1) \ . \quad (9)$$

Table 3 contains the Mg-Fe partitioning data at 1600 °C in a wide compositional range (12.7 to 85.4 mol% Mg_2SiO_4 in spinel). Using Eq. (9), we can estimate W_G^{sp}, W_G^{sp}, and ΔG° at a given pressure-temperature condition by the least-squares method from the partitioning data. However, it should be remembered that the partitioning experiments at 1600 °C were performed at some different pressures of 17–21.3 GPa, because stability of spinel solid solution is limited in a compositional range of, for example, about 10–65 mol% Mg_2SiO_4 at 19 GPa and 1600 °C, due to the stability of the β-phase in the Mg-rich composition and the mixture of magnesiowüstite and stishovite in the Fe-rich side (Akaogi et al. 1989, 1998). Therefore, it is necessary to correct all the data to the same pressure. We corrected the data to 19 GPa, which was close to the average pressure of the runs at 17–21.3 GPa. For each run at pressure lower or higher than 19 GPa at 1600 °C, a correction was made by adding $\int_P^{19GPa} \Delta V(P', T)dP'$, where P was the run pressure and ΔV was volume change of Eq. (2), because of $(\partial\Delta G/\partial P)_T = \Delta V$. This correction was calculated by the same method as that in the following section, and was within about 1.6 kJ mol^{-1}. Figure 4 shows the relationship between X^{sp}_{Mg} and corrected values of $-RTln\ K_D$. Then, the parameters W_G^{sp}, W_G^{mw}, and ΔG° at 19 GPa and 1600 °C were simultaneously calculated by the least-squares method. The obtained values of W_G^{sp} and W_G^{mw} were, respectively, 3.4 ± 1.5 and 13.9 ± 1.4 kJ mol^{-1}, and ΔG° was 15.0 ± 0.7 kJ mol^{-1}.

Calculation of spinel dissociation boundaries

The transition boundaries from spinel to magnesiowüstite and stishovite in the system Mg_2SiO_4-Fe_2SiO_4 are calculated as follows. The equilibrium where spinel coexists with magnesiowüstite and stishovite is expressed as

$$Mg_2SiO_4(sp) = 2MgO(mw) + SiO_2(st) \ . \quad (10)$$

The other equilibrium is expressed as

$$Fe_2SiO_4(sp) = 2FeO(mw) + SiO_2(st) \ . \quad (11)$$

At equilibrium, we have

$$\mu^{sp}_{Mg_2SiO_4} = 2\mu^{mw}_{MgO} + \mu^{st}_{SiO_2} \quad (12)$$

$$\mu^{sp}_{Fe_2SiO_4} = 2\mu^{mw}_{FeO} + \mu^{st}_{SiO_2} \ . \quad (13)$$

The activity of stishovite is taken to be unity, because stishovite can be regarded as a pure SiO_2 phase. Using Eqs. (4), (12), and (13), we have:

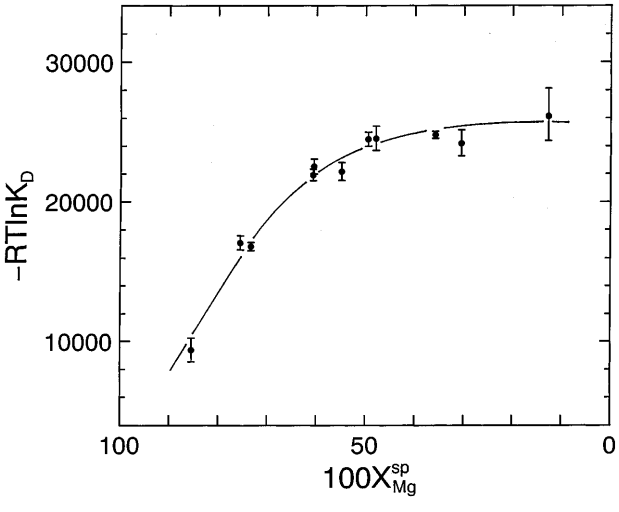

Fig. 4 Relationship between $-RTlnK_D$ and X^{sp}_{Mg} at 19 GPa and 1600 °C. The K_D is the Mg-Fe partition coefficient between spinel and magnesiowüstite defined by $(X^{sp}_{Fe}/X^{sp}_{Mg})/(X^{mw}_{Fe}/X^{mw}_{Mg})$. A *solid curve* was calculated by the least-squares fitting to the data

$$\Delta H_{Mg}(0,T) - T\Delta S_{Mg}(0,T) + \int_{1atm}^{P} \Delta V_{Mg}(P',T)dP' + RT\ln\left[\left(a_{MgO}^{mw}\right)^2 / a_{Mg_2SiO_4}^{sp}\right] = 0 \quad (14)$$

$$\Delta H_{Fe}(0,T) - T\Delta S_{Fe}(0,T) + \int_{1atm}^{P} \Delta V_{Fe}(P',T)dP' + RT\ln\left[\left(a_{FeO}^{mw}\right)^2 / a_{Fe_2SiO_4}^{sp}\right] = 0 \ , \quad (15)$$

where $\Delta H_{Mg}(0,T)$ and $\Delta S_{Mg}(0,T)$ are enthalpy and entropy changes for Eq. (10) at T and 1 atm, and $\Delta V_{Mg}(P,T)$ is volume change for Eq. (10) at P and T. The compositions of coexisting spinel and magnesiowüstite are calculated by solving Eqs. (14) and (15) simultaneously with the activity-composition relationships for spinel and magnesiowüstite solid solutions, using Eqs. (6)–(8).

To calculate the effect of temperature on enthalpy and entropy changes in Eqs. (14) and (15), we use heat capacity differences $\Delta C_p(T)$ for the reactions (10) and (11), respectively, by

$$\Delta H(0,T) = \Delta H(0,T_0) + \int_{T_0}^{T} \Delta C_p(T')dT' \quad (16)$$

$$\Delta S(0,T) = \Delta S(0,T_0) + \int_{T_0}^{T} \Delta C_p(T')/T'dT' \ , \quad (17)$$

where T_0 is the reference temperature. Pressure and temperature effects on molar volume in Eqs. (14) and (15) are corrected as follows. Molar volume at T and 1 atm is calculated as

$$V_0 = V(0,298)\exp\left[\int_{298}^{T} \alpha(T')dT'\right] \ , \quad (18)$$

where V_0 is molar volume at T and 1 atm, V(0,298) is that at 298 K and 1 atm, and $\alpha(T)$ is thermal expansivity at T and 1 atm. To calculate molar volume at P and T, the third-order Birch-Murnaghan equation of state is used,

$$P = (3/2)K_T\left[(V_0/V)^{7/3} - (V_0/V)^{5/3}\right] \times \left\{1 - (3/4)(4 - K_T')\left[(V_0/V)^{2/3} - 1\right]\right\} \ , \quad (19)$$

where V is molar volume at P and T. The K_T and K_T' are isothermal bulk modulus and its pressure derivative, respectively. The bulk modulus at T is calculated, using its temperature derivative $(\partial K_T/\partial T)_P$, as

$$K_T = K_{T,298} + (\partial K_T/T)_p(T - 298) \ , \quad (20)$$

where $K_{T,298}$ is isothermal bulk modulus at 298 K.

Table 4 summarizes molar volumes, thermal expansivities, bulk moduli, their pressure- and temperature-derivatives, and heat capacities used in the thermodynamic calculation. Akaogi et al. (1998) obtained the enthalpy and entropy changes for Eqs. (10) and (11), based on calorimetric measurements combined with phase equilibrium data: $\Delta H(0,298) = 56.74 \pm 5.75$ kJ mol^{-1}, $\Delta S(0,298) = -4.6 \pm 1.0$ J mol^{-1} K^{-1} for (10), and $\Delta H(0,298) = 63.33 \pm 3.11$ kJ mol^{-1}, $\Delta S(0,298) = -5.6 \pm 2.4$ J mol^{-1} K^{-1} for (11). To further constrain the enthalpy and entropy data, we use the free energy change of Eq. (2) obtained from the Mg-Fe partitioning data. By Eqs. (5), (14), and (15), the ΔG° is related with the enthalpy, entropy, and volume changes for Eqs. (10) and (11), as follows:

$$\Delta G^\circ = 1/2\left[\Delta H_{Mg}(0,T) - T\Delta S_{Mg}(0,T) + \int_{1atm}^{P} \Delta V_{Mg}(P',T)dP'\right]$$

Table 4 Molar volumes, thermal expansivities, heat capacities, bulk moduli and their pressure- and temperature-derivatives of the phases in the system MgO-FeO-SiO_2

Phase	V(0,298) (cm^3 mol^{-1})	$\alpha = a + bT + cT^{-2}$ (K^{-1})			K_T (GPa)	K_T'	$(\partial K_T/\partial T)_P$ (GPaK^{-1})	$C_p = A + BT^{-0.5} + CT^{-2} + DT^{-3}$ (J mol^{-1} K^{-1})			
		a × 10^5	b × 10^9	c × 10				A × 10^{-2}	B × 10^{-3}	C × 10^{-6}	D × 10^{-8}
Mg_2SiO_4 sp	39.487[a]	2.448	4.056	−6.029[b]	182.6[b]	5.0[c]	−0.0284[b]	2.178	−1.543	−0.569	−4.192[i]
Fe_2SiO_4 sp	42.040[d]	2.455	3.591	−3.703[e]	192.0[f]	5.0[g]	−0.0284[g]	2.813	−2.902	0.0	5.041[i]
MgO per	11.248[h]	3.753	7.941	−7.787[i]	160.3[j]	4.1[j]	−0.0272[k]	0.586	−0.189	−1.664	0.234[h]
FeO wü	12.250[i]	1.688	2.040	0.190[i]	153.0[l]	4.9[l]	−0.0272[m]	0.857	−0.871	0.0	3.954[i]
SiO_2 st	14.014[h]	1.053	9.031	1.220[i]	314.0[n]	5.1[o]	−0.0470[e]	0.858	−0.346	−3.605	4.511[p]

[a] Ito and Yamada (1982)
[b] Meng et al. (1993)
[c] Rigden et al. (1991)
[d] Marumo et al. (1977)
[e] Fei et al. (1991)
[f] Sato (1977) and Bass et al. (1981)
[g] Same as Mg_2SiO_4 spinel
[h] Robie et al. (1978)
[i] Saxena et al. (1993)
[j] Jackson and Niesler (1982)
[k] Anderson et al. (1992)
[l] Jackson et al. (1990)
[m] Same as MgO
[n] Weidner et al. (1982)
[o] Rigden et al. (1994)
[p] Akaogi et al. (1995)

$$-1/2\left[\Delta H_{Fe}(0,T) - T\Delta S_{Fe}(0,T) + \int_{1atm}^{P} \Delta V_{Fe}(P',T)dP'\right] . \quad (21)$$

Using the parameters in Table 4, the right-hand side of Eq. (21) at 19 GPa and 1600 °C was calculated with the above values of $\Delta H(0,298)$ and $\Delta S(0,298)$ for Eqs. (10) and (11) within the uncertainties. Then, we chose the upper (or lower) bounds of the enthalpy and entropy changes [$\Delta H(0,298) = 62.49$ kJ mol^{-1}, $\Delta S(0,298) = -5.6$ J mol^{-1} K^{-1} for (10), $\Delta H(0,298) = 66.44$ kJ mol^{-1}, $\Delta S(0,298) = -3.2$ J mol^{-1} K^{-1} for (11)] to calculate the transition boundaries, because this set gave the value of ΔG^0 at 19 GPa and 1600 °C, 15.64 kJ mol^{-1}, which was consistent with 15.0 ± 0.7 kJ mol^{-1} obtained from the partitioning data.

The dissociation boundaries of spinel into magnesiowüstite and stishovite were calculated by the above method, using the above set of $\Delta H(0,298)$ and $\Delta S(0,298)$ and the parameters in Table 4 together with the interaction parameters of spinel and magnesiowüstite, $W_G^{sp} = 3.4 \pm 1.5$ kJ mol^{-1} and $W_G^{mw} = 13.9 \pm 1.4$ kJ mol^{-1}, obtained in the previous section. When the calculated boundaries were compared with those determined experimentally at 1400 and 1600 °C, we found that the lower bounds of W_G^{sp} and W_G^{mw} gave most consistent boundaries with the experimental data at the two different temperatures. The boundaries calculated using $W_G^{sp} = 1.9$ kJ mol^{-1} and $W_G^{mw} = 12.5$ kJ mol^{-1} are shown in Fig. 5. The calculated boundaries agree with the experimental data within about 3 mol% in Fe_2SiO_4 or within about 0.3 GPa. This suggests that the thermodynamic data set with its uncertainties gives the calculated boundaries consistent with the experimental data at both 1400 and 1600 °C. Although the partitioning data at 1600 °C in the Fe-rich composition were used to derive the interaction parameters, it should be noted that no data at 1400 °C were used to obtain the W_G^{sp} and W_G^{mw}. The calculated boundaries show that the dP/dT slope of the transition boundary from spinel to magnesiowüstite and stishovite is negative.

The interaction parameter W_G may be expressed as

$$W_G = W_H - TW_S + PW_V , \quad (22)$$

where W_H is excess enthalpy of mixing at 1 atm, and W_S and W_V are, respectively, excess entropy and volume of mixing of the solid solution. Akaogi et al. (1989) carried out heat of solution measurements of spinel solid solutions, and applied the symmetric regular solution model to the data. They obtained the W_H^{sp} to be 3.9 kJ mol^{-1} for one cation site basis. The linear molar volume-composition relationship of spinel solid solution indicates that W_V^{sp} can be regarded as zero (Akaogi et al. 1989). Therefore, the obtained value of W_G^{sp} (1.9 kJ mol^{-1}) suggests that the W_G^{sp} decreases with temperature, and the W_S^{sp} was estimated as about 1 J mol^{-1} K^{-1}, though its error was large due to the large uncertainty of W_G^{sp}. The activity measurements of magnesiowüstite solid solutions showed that the W_G^{mw} is approximately 14 kJ mol^{-1} at 1 atm (Hahn and Muan 1962; Williams 1971; Srecec et al. 1987). When we compare the above W_G^{mw} at 16 GPa with this value at 1 atm, it may be suggested that pressure dependence of W_G^{mw} is very small.

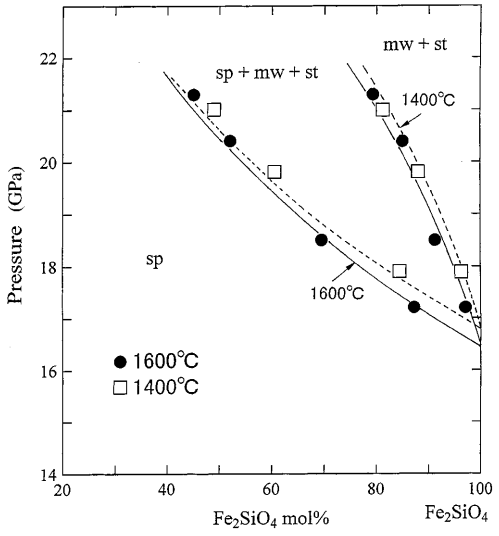

Fig. 5 Comparison of the calculated boundaries for dissociation of spinel with the equilibrium compositions of spinel and magnesiowüstite determined by the partitioning experiments in the system Mg_2SiO_4-Fe_2SiO_4. *Squares* and *circles* show the compositions at 1400 and 1600 °C, respectively; *sp* spinel; *mw* magnesiowüstite; *st* stishovite

Finally, the dissociation boundary of Fe_2SiO_4 spinel is discussed here. Previous studies on the boundary show considerable disagreement. Kawada (1977) reported a positive slope boundary, while Ohtani (1979) showed a boundary with a negative slope. Their dissociation pressures differ by about 3 GPa at 1100 °C. Such a large discrepancy presumably could not be explained only by difference in the pressure calibration. Sluggish reaction of dissociation of Fe_2SiO_4 spinel would be one of the important factors to make the difference in the transition boundaries, because a large amount of spinel was observed together with wüstite and stishovite at about 1100–1600 °C in a wide pressure range beyond the proposed transition boundaries (Kawada 1977; Ohtani 1979). Katsura et al. (1998) redetermined the dissociation boundary, using iron chloride as a catalyst to enhance the reaction rate. They found that complete dissociation of spinel occurred at 937–1337 °C, and their dissociation boundary determined by the normal and reverse runs had a zero slope. Figure 6 shows their experimental data together with our calculated boundary using the above enthalpy and entropy data for the reaction (11) by Akaogi et al. (1998) and the physical properties in Table 4. Our calculated boundary has a negative slope of −1.5 ± 0.6 MPa K^{-1}, the uncertainty

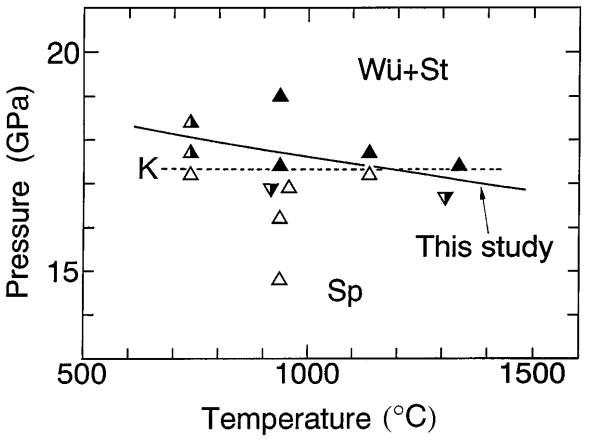

Fig. 6 Dissociation boundaries of Fe_2SiO_4 spinel to wüstite and stishovite. The *solid line* is the calculated boundary in this study. *Dotted line labeled K* and experimental data points (*triangles* and *reverse triangles*) are from Katsura et al. (1998). The *triangles* and the *reverse triangles* represent normal and reverse runs, respectively. *Filled* and *open symbols* show the presence of wüstite + stishovite and spinel, respectively, in the run products. *Half-filled symbols* represent the presence of the three phases in the run products; *sp* spinel; *wü* wüstite; *st* stishovite

of which is derived from the errors of the enthalpy and entropy data for Eq. (11). The Mg-Fe partitioning data in Fig. 2 and the calculated boundaries in Fig. 5 suggest that the dP/dT slope of the dissociation boundaries of spinel to magnesiowüstite and stishovite becomes more negative with increasing Fe_2SiO_4 component. Katsura et al. (1998) calibrated the pressure only at 1137 °C, and temperature dependence of the calibrated pressure was not considered. This might explain, at least in part, the discrepancy in the slope between our studies and those of Katsura et al. Further experimental study will be necessary to determine more accurately the dissociation boundary of Fe_2SiO_4 spinel.

Acknowledgements We are very grateful to T. Ishii for his help in EPMA analysis and to T. Katsura for sending us a preprint of his paper. Comments by two anonymous reviewers were useful to improve the manuscript. This work was supported in part by Grants-in-Aid from Ministry of Education, Science, and Culture, Japan.

References

Akaogi M, Navrotsky A (1984) The quartz-coesite-stishovite transformations: new calorimetric measurements and calculation of phase diagrams. Phys Earth Planet Inter 36: 124–134

Akaogi M, Ito E, Navrotsky A (1989) Olivine-modified spinel-spinel transitions in the system Mg_2SiO_4-Fe_2SiO_4: calorimetric measurements, thermochemical calculations, and geophysical applications. J Geophys Res 94: 15671–15685

Akaogi M, Yusa H, Shiraishi K, Suzuki T (1995) Thermodynamic properties of α-quartz, coesite, and stishovite and equilibrium phase relations at high pressures and high temperatures. J Geophys Res 100: 22337–22347

Akaogi M, Kojitani H, Matsuzaka K, Suzuki T, Ito E (1998) Postspinel transformations in the system Mg_2SiO_4-Fe_2SiO_4: element partitioning, calorimetry, and thermodynamic calculation. In: Manghnani MH, Yagi T (eds) High pressure-temperature research: properties of earth and planetary materials. Am Geophys Union, pp 373–384

Anderson OL, Isaak D, Oda H (1992) High temperature elastic constant data on minerals relevant to geophysics. Rev Geophys 30: 57–90

Bass JD, Liebermann RC, Weidner DJ, Finch SJ (1981) Elastic properties from acoustic and volume compression experiments. Phys Earth Planet Inter 25: 140–158

Fei Y, Mao HK, Mysen BO (1991) Experimental determination of element partitioning and calculation of phase relations in the MgO-FeO-SiO_2 system at high pressure and high temperature. J Geophys Res 96: 2157–2169

Hahn WC, Muan A (1962) Activity measurements in oxide solid solutions: the system "FeO"-MgO in the temperature range 1100 to 1300 °C. Trans Met Soc Am Inst Met Eng 224: 416–420

Ito E, Takahashi E (1989) Postspinel transformations in the system Mg_2SiO_4-Fe_2SiO_4 and some geophysical implications. J Geophys Res 94: 10637–10646

Ito E, Yamada H (1982) Stability relations of silicate spinels, ilmenites and perovskites. In: Akimoto S, Manghnani MH (eds) High-pressure research in geophysics. Center Acad Publ Japan, Tokyo, pp 405–419

Jackson I, Niesler H (1982) The elasticity of periclase to 3 GPa and some geophysical implications. In: Akimoto S, Manghnani MH (eds) High-pressure research in geophysics. Center Acad Publ Japan, Tokyo, pp 93–113

Jackson I, Khanna SK, Revcolevschi A, Berthon J (1990) Elasticity, shear-mode softening and high-pressure polymorphism of wüstite ($Fe_{1-x}O$). J Geophys Res 95: 21671–21685

Katsura T, Ito E (1989) The system Mg_2SiO_4-Fe_2SiO_4 at high pressures and temperatures: precise determination of stabilities of olivine, modified spinel, and spinel. J Geophys Res 94: 15663–15670

Katsura T, Ueda A, Ito E, Morooka K (1998) Postspinel transition in Fe_2SiO_4. In: Manghnani MH, Yagi T (eds) High pressure-temperature research: properties of earth and planetary materials. Am Geophys Union, pp 435–440

Kawada K (1977) The system Mg_2SiO_4-Fe_2SiO_4 at high pressures and temperatures and the earth's interior. Ph D Thesis, Univ of Tokyo

Liu J, Topor L, Zhang J, Navrotsky A, Liebermann RC (1996) Calorimetric study of the coesite-stishovite transformation and calculation of the phase boundary. Phys Chem Miner 23: 11–16

Marumo F, Isobe M, Akimoto S (1977) Electron-density distribution in crystals of γ-Fe_2SiO_4 and γ-Co_2SiO_4. Acta Crystallogr Ser B 33: 713–716

McCammon C, Peyronneau J, Poirier JP (1998) Low ferric iron content of (Mg,Fe)O at high pressures and temperatures. Geophys Res Lett 25: 1589–1592

Meng Y, Weidner DJ, Gwanmesia GD, Liebermann RC, Vaughan MT, Wang Y, Leinenweber K, Pacalo RE, Yeganeh-Haeri A, Zhao Y (1993) In situ high P-T X-ray diffraction studies on three polymorphs (α, β, γ) of Mg_2SiO_4. J Geophys Res 98: 22199–22207

Ohtani E (1979) Melting relation of Fe_2SiO_4 up to about 200 kbar. J Phys Earth 27: 189–208

Rigden SM, Gwanmesia GD, Fitz Gerald JD, Jackson I, Liebermann RC (1991) Spinel elasticity and seismic structure of the transition zone of the mantle. Nature 354: 143–145

Rigden SM, Li B, Liebermann RC (1994) Elasticity of stishovite at high pressures. Eos Trans Am Geophys Union 75, p 596

Robie RA, Hemingway BS, Fisher JR (1978) Thermodynamic properties of minerals and related substances at 298.15 K and 1 bar (10^5 pascals) pressure and higher temperatures. US Geol Surv Bull 1452, 456 pp

Sato Y (1977) Equation of state of mantle minerals determined through high-pressure X ray study. In: Manghnani MH, Akimoto S (eds) High-pressure research: applications in geophysics. Academic Press, New York, pp 307–323

Saxena SK, Chatterjee N, Fei Y, Shen G (1993) Thermodynamic data on oxides and silicates. Springer, Berlin Heidelberg New York, 428 pp

Srecec I, Ender E, Woermann E, Gans W, Jacobsson E, Eriksson G, Rosen E (1987) Activity-composition relations of the magnesiowüstite solid solutions series in equilibrium with metallic iron in the temperature range 1050–1400 K. Phys Chem Miner 14: 492–498

Thompson JB (1967) Thermodynamic properties of simple solutions. In: Abelson PH (ed) Researches in geochemistry. Wiley, New York, pp 340–361

Weidner DJ, Bass JD, Ringwood AE, Sinclair W (1982) The single-crystal elastic moduli of stishovite. J Geophys Res 87: 4740–4746

Williams R (1971) Reaction constants in the system Fe-MgO-SiO_2-O_2 at 1 atm between 900° and 1300 °C: experimental results. Am J Sci 270: 334–360

Yagi T, Bell PM, Mao HK (1979) Phase relations in the system MgO-FeO-SiO_2 between 150 and 700 kbar at 1000 °C. Carnegie Inst Washington Year Book 78: 614–618